

# A Novel Entry, Descent and Landing Architecture for Mars Landers

Malaya Kumar Biswal.M<sup>1</sup>, Ramesh Naidu.A<sup>2</sup>

Department of Physics, Pondicherry University, Puducherry – 605014, India

**Abstract.** Landing robotic spacecrafts and humans on the surface of Mars has become one of the inevitable technological necessity for humans. To accomplish this intention, we need to land enormous number of cargoes, crewed modules, return vehicles and scientific laboratories on Mars. In this entailing condition, there are many incidences of crash landing leading to complete demolition of lander modules. Crash landing occurs under numerous circumstances. Significant problems were loss of communication, onboard command error, lander malfunction, software problem and premature EDL performance. Moreover, existence of deformable shock absorbers like Aluminium honeycomb and crushable carbon fibers in landing gears are not feasible for high scale mass and crewed landing. Consequently, it may cause impairment of landing module. Further, while evaluating the interim EDL performance, landing and switching EDL events within a limited span of 5 to 8 minutes appears to be the most challenging task. Scrutinizing this concern, we propose a novel shock absorbing landing gear system that will be more achievable for large scale and frequent landing missions. This paper relies on theoretical proposition of practical design of landing gear system and we expect that, subject to any obstruction in EDL sequence, this mechanical system will enable soft-landing thereby increasing the probability of success in forthcoming landing missions. Hence, our ultimate aim is to protect lander modules and their instruments during the course of landing.

**Keywords:** Aerocapture, Hydraulics, Inflatable, Landing module, Retropropulsive

**Major Identified Problems:** Loss of communication, command error, Lander malfunction, software problem, premature EDL performance

## 1 Introduction

Making humans multi-planetary species has become an ultimate goal to human race [1]. To meet this goal, we need to land large number of scientific, cargo and manned landers on Mars. Under these circumstances, there have been many instances of crash landing of landers due to hard impact which leads to failure of missions. Previously used landers like Venera and Viking utilized shock absorbing materials such as Aluminium foam and Aluminium honeycomb which possess high energy absorption efficiency [2, 3]. Soviet landers made use of foam plastic as their primary shock absorber [4]. In spite of using efficient shock absorbers, some landers fail to perform touchdown phase. Since, the EDL time for Mars is too short i.e., 5-8 minutes, all the EDL sequences should be performed perfectly within this short duration [5]. To address this technological challenge we propose a novel hybrid shock absorber (compression spring integrated with hydraulics) to achieve soft-landing, excluding any obstruction in EDL performance. Hence our ultimate aim is to protect the lander module and its instruments from abrupt impact during landing on the surface of Mars.

---

\* Department of Physics, Pondicherry University, Puducherry – 605014, India.

E-mail address: mkumar97.res@pondiuni.edu.in, rameshnaidu.phy@pondiuni.edu.in

## 2. Past and Present Lander Missions

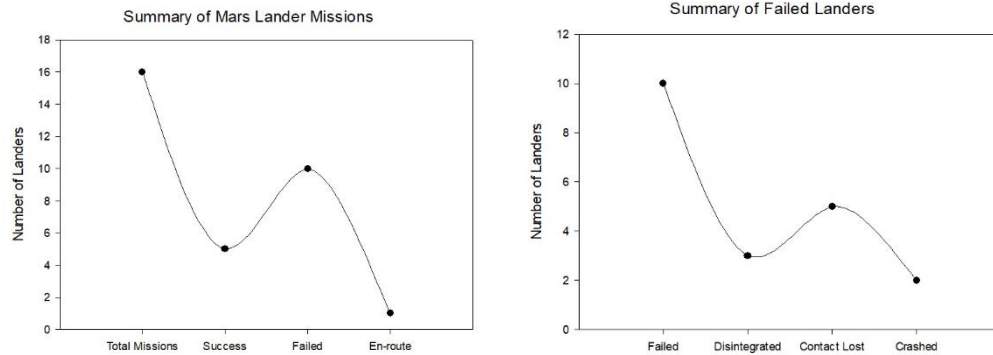


**Fig.1** Summary of Failed Landers

The first step to Mars exploration was initiated by Soviet Union in late 1962, when Mars 2MV-3 No.1 carried Molniya rocket. This mission ended in failure, disintegrated in low earth orbit, owing to persistent issues related to launcher [6]. The USSR made a second attempt to land on Mars with Mars 2 lander in 1971. After the Mars 2 lander crashed on the Martian surface, the succeeding initiative Mars 3, an unmanned space probe performed soft-landing whose data transmission lasted for twenty seconds [4]. Similarly, in 1973 Russian's attempted to land on Mars with Mars 5, Mars 6 and Mars 7, all of them remained unsuccessful. Mars 5 launched on July 25, 1973, arrived on Mars orbiter on Feb. 12th, 1974, but lasted only a few days. Similarly as lander failed due to a fast impact Mars 6 was unsuccessful while Mars 7 failed to perform atmospheric entry as it missed the planet [4]. In 1975, NASA's first attempt to land on Mars with twin Viking landers (Viking-1 and Viking-2) brought them success. They performed excellent landing with successful accomplishment of mission goal [3]. In 1988, Soviet Union made fourth attempt to land on Mars with Phobos landers (Phobos-1 and Phobos-2). The mission of Phobos 1 was unsuccessful due to communication issues before reaching its destination. Phobos-2 entered Mars atmosphere successfully but the solar panel failed to deploy [4]. In 1996, United States achieved its second success when the landing of Mars Pathfinder on the surface of Mars with a mini-rover. Its new parachute deployment and air-bag landing system, helped in achieving soft-landing on to the Martian surface. Meanwhile, Soviet's Mars96 lander failed due to malfunctioning of on board computer and upper-stage booster and disintegration in LEO. Subsequent lander missions such as Mars Polar Lander in 1999, which lost its contact prior to landing and the Mars Phoenix Lander in 2007 made successful landing and achieved their mission goal. In 2003, European Space Agency's first attempt to land on Mars (Beagle-2 lander), performed successful landing. It lost its communication after soft-landing and remained unsuccessful. They made a second attempt to land on Mars with Schiaparelli EDM lander which performed successful entry into the Martian atmosphere. As a result of premature deployment of parachute due to the fatal error in guidance and control system, Schiaparelli crashed on Martian surface. It measured and transmitted real time data of Martian atmosphere that helped to conclude the partial success of mission [7]. Recently, in May 2018, NASA had launched InSight Mars Lander which is on its trajectory phase to Mars. It is estimated that the lander would attempt soft-landing by November 2018.

### 3. Crashed Landers Report

In November 1971, Mars 2 lander entered the Mars atmosphere at a wide angle and crashed on the Martian surface due to wrong command issued by the on-board computers [4]. In December 1999, Mars Polar Lander and Deep 2 Space Penetrator lost communication prior to landing [8]. Meanwhile, in October 2016, Schiaparelli EDM lander crashed on the surface due to premature deployment of parachute landing system [7].

**Table 1** Comparative EDL Summary of Mars Landers

Parameters	Mars 2	Mars 3	Mars 6	Mars 7	Viking-1	Viking-2	Phobos 1 and 2	MPF
Entry Mode	direct	direct	direct	direct	orbit	orbit	direct	direct
Entry Velocity					4.61	4.74	-	7.26
Relative Entry Velocity	6.0	5.7	5.6	1.2	4.42	4.48	-	7.48
Peak Heat Velocity					4.02	4.0	-	6.61
Aeroshell	120° break cone	120° break cone	120° break cone	120° break cone	70°Sphere Cone	70°Sphere Cone	-	70°Sphere Cone
Base Area					9.65	9.65	-	5.52
Ballistic Coefficient					64	64	-	62.3
Entry Mass	1210	1210	635	635	992	992	2600	584
Mass	358	358	635	635	590	590	6220	361
Aeroshell Diameter	3.2	3.2	3.2	3.2	3.5	3.5	-	2.65
Parachute Diameter					16	16	-	12.5
Parachute Drag					0.67	0.67	-	0.4
Lift/ Drag ratio					0.18	0.18	-	0
Vertical Velocity					2.4	2.4	-	12.5
Landing Legs	Ring	Ring	Ring	Ring	3	4	-	0
Touchdown Mass	358	358	635	635	590	590	-	360
Touchdown Velocity			0.06		2.4	2.4	-	12.5
Attenuator Material	Foam Plastic	Foam Plastic	Foam Plastic	Foam Plastic	Aluminium honeycomb	Aluminium honeycomb	Foam Plastic	Air-bags
Landing Site	45°S 47°E	45°S 202°E	23.90°S 19.42°W	-	22.27°N 47.95°W	47.64°N 225.71°W	-	19°7N 33°13W
MOLA					-3.5	-3.5	-	-2.5
References	[4,33,34]	[4,33,34]	[4,33,34]	[4,33,34]	[6,34,35]	[6,34,35]	[36]	[6,37,34]

**Table 1** (Continued)

Parameters	Mars 96	Mars 96 Penetrator	MPL	Beagle 2	Deep 2 Space	Phoenix Lander	Schiaparelli	InSight
Entry Mode	direct	Direct	direct	direct	direct	direct	direct	direct
Entry Velocity	5.75	4.9	6.91	5.63		5.59		
Relative Entry Velocity	4.9	4.6	6.80	5.40	6.9	5.67	5.83	6.3
Peak Heat Velocity		-		4.70	5.94			
Aeroshell	Blunt Ended Cone	Blunt Ended Cone	70°Sphere Cone	60° Sphere Cone	45° Sphere Cone	70°Sphere Cone	70°Sphere Cone	70°Sphere Cone
Base Area				0.62				
Ballistic Coefficient			65	69.9	36.2	70	82	
Entry Mass	120.5	45	487	72.7		603	577	608
Mass	3159	88	583	33.2	2.4		577	727
Aeroshell Diameter	1	0.29	2.4	0.93		2.65	2.4	6.1
Parachute Diameter	-			10.4		11.5	12	
Parachute Drag	-			0.92		0.62		
Lift/ Drag ratio	-			2°		0	0	
Vertical Velocity	0.02	0.075	2.4			2.4		2.3
Landing Legs	Ring		3	0	0	3	0	3
Touchdown Mass	30.6	4.5	423.6	33.2	2.4	364	280	360
Touchdown Velocity	0.02	0.075	2.4		0.17	2.4	0.15	
Attenuator Material	Air-bags	Inflatable Ballute	Aluminium honeycomb	Air-bags	Hard Lander	Crushable	Crushable carbon fiber	Crushable
Landing Site	41°31N 153°77W	-	76°S 195°W	11.53°N 90.43°E	73°S 210°W	68.22°N 125.7°W	6.208°W 2.052°S	4.5°N 135.0°E
MOLA			-3.0			-3.5	1.45	-2.5
References	[38,39,40]	[40]	[41,34,49]	[42,43,44]	[6,34]	[6,34,35]	[45,46]	[9,47,48]

#### 4. Landing Challenges

For a successive landing of lander, the mission has to address several challenges arising due to thickness of Martian atmosphere, low elevation, short EDL period and surface hazards which include the distribution of large sized rocks, craters, terrains and devil dust storms. Especially, legged landers have rock hazards as their largest challenge and the EDL time (5-8 minutes) is not sufficient to perform all the entry, descent and landing phase accurately [5]. Past landers used Aluminium honeycomb, foam plastic, air bags and crushable carbon fibers for impact attenuation. These attenuators will limit the landing mass to 0.6 ton [5]. In future manned lander missions, it is necessary to land large cargoes, habitat and rockets. In landing large masses, several factors are taken into consideration. Factors such as diameter of aeroshell, parachute and ballistic coefficient are limited.

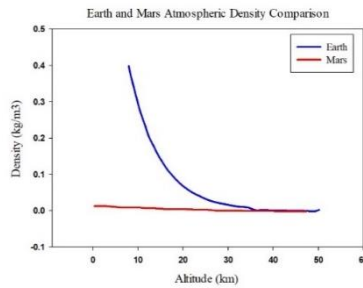


**Fig.2** Atmospheric density comparison Earth-Mars [6]

For a successful soft-landing with currently available technology,

- Masses should lie between 0.6 to 0.9 ton
- Ballistic coefficient should be  $<35 \text{ kg/m}^2$
- The diameter of aeroshell should be  $<4.6 \text{ m}$  (70-deg spherical cone aeroshell)
- The parachute diameter should be limited to  $<30 \text{ m}$  with Mach 2.7 disk-gap band parachute
- Need to use supersonic retro propulsion systems
- Need to enter the lander from orbit [6]

#### 5. Scientific Background

Past landers were configured with Aluminium foam, Aluminium honeycomb and foam plastic to absorb impact force during the course of landing. Moreover, landers like Mars Pathfinder and Beagle-2 lander used additional air-bags for impact distribution. Further, in the MPL and Mars Phoenix landers retro propulsive system was deployed to scale down the vertical velocity. Despite these technologies interventions, crash landing occurs due to numerous factors. Therefore, in this paper we are proposing hybrid shock absorber which utilize the mechanism of hydraulics and helical compression spring to absorb shock during landing phase. In addition to this, we incorporated hydraulic drive system which is supposed to work only if the pressure of the secondary unit exceeds beyond a predetermined level.

## 6. Methods and Materials

### a. Helical Compression Spring

In primary unit, we prefer to use helical-compression springs as primary shock absorbing material. Compression spring has the ability to store and release energy substantially delivered by the lander in axial direction during terminal descent phase. It is supposed to absorb instant shock and deliver to the secondary unit. The strength of the spring depends on spring constant ( $k$ ) which ultimately relies on mass and forces exerted by lander modules. Subject to the type of material, the strength of the compression spring varies. Among various spring alloys, we propound to use a specific type Silicon-Chromium Oil Tempered Wire (SWOSC-V) named so by Japanese Society of Spring Engineers [10]. It has high tensile strength ranging from 2010 MPa to 2160 MPa having temperature tolerance ranging from 400°C to 450°C [10] which is most suitable for high mass landers. Hence, compression spring might play a significant role in maintaining balanced forces between lander module and planetary surface of Mars. It also possesses the following mechanical characteristics.



**Fig.3** Compression Spring

**Table.2** Mechanical Characteristics of spring [10]

Characteristics	Value
Yield point	1820
Elastic Limit	1690
Yield Ratio	90.7
Elastic Limit Ratio	83.9
Young Modulus	203 GPa
Tensile Strength	2010 -2160 MPa
Temperature Range	400°C to 450°C
Holding Time	20 – 30 minutes

### b. Hydraulic Fluid

Hydraulic fluids such as mineral oil, water, emulsions, water-based glycols, synthetic fluids are ecologically acceptable fluids. Among these fluids, most of the hydraulic system uses mineral oil as their major constituent of hydraulic fluid. We prefer to use particular type HV-Mineral oil with addition of extra additives such as viscosity improvers. HV-Mineral oil comprises of HM-Type mineral oil plus extra additives. It can accomplish all the requirements except 'fire-resistance' [11] with fluid density range from 0.8 to 0.9 g/ml [12].

## 7. Methods

### a. Primary Unit – Spring Damper

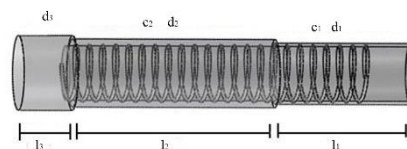


**Fig.4.** Spring Damper

Primary unit will be our principal shock absorber. It comprises of spring compartment and helical compression spring (Si-Cr) of length  $l_s$ . It can be compressed like hydraulic system due to retractable setup of two cylinders of different diameters. It has a base cap of length and diameter ( $l_3, d_3$ ) and cylinders of length ( $l_1, l_2$ ) and diameter ( $d_1, d_2$ ). The length of the spring can be defined as  $l_s = (l_1 - l_4) + l_2$  m. The unit is compressible according to defined

spring constant and force delivered. Its geometrical structure is determined by the mass, force and geometry of landers. This unit is capable of absorbing impact force expeditiously.

### b. Secondary Unit – Hydraulic Damper

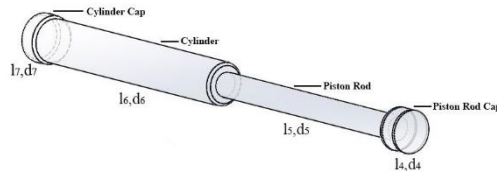


**Fig.5** Hydraulic Damper

The hydraulic shock absorber has a piston rod cap of diameter  $d_4$  and length  $l_4$ , piston rod is about length  $l_5$  and diameter  $d_5$ . It also has cylindrical body of length  $l_6$  and diameter  $d_6$  with a cylindrical cap attached whose diameter is  $d_7$  and length  $l_7$ . Hydraulic shock absorber can be employed to absorb shock with the help of hydraulic accumulator attached to that system. It has been used for pneumatic systems where the impact force and vibration are the prime reason for the failure. Hydraulic systems are the best for energy dissipation at a moderate rate and they have been good systems for shock absorption as well as shock attenuation. The key advantage of hydraulic system is that it has the ability of rapid energy absorption and moderate energy dissipation. Here in our shock absorption system, we propose to use hydraulic cylinder as secondary unit. The impact energy from the primary unit (Spring-compartment) is absorbed and dissipated slowly by pushing the piston upwards. At this stage, the fluid inside the chamber is exposed to a huge pressure which can be measured by a pressure sensor present inside it. If the pressure exceeds its critical level, the pressure sensor gets activated which will be sending a signal so that pressure valve might open. Following this stage, the fluid might pass slowly into another compartment (i.e.,) tertiary unit through a fluid pass tube.

### c. Tertiary Unit – Energy Dissipater

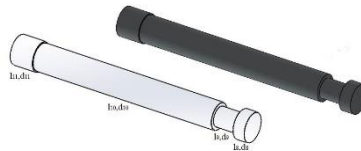


**Fig.6** Energy Dissipater

The energy dissipater consists of piston rod cap of length of  $l_8$  and diameter  $d_8$ , piston rod of length of  $l_9$  and  $d_9$ , cylindrical body of length  $l_{10}$  and diameter  $d_{10}$  with an attached cylinder cap of length  $l_{11}$  and diameter  $d_{11}$ . The hydraulic fluid which passed from secondary unit will start to exert pressure on the hydraulic piston in tertiary unit. As a result, the fluid will drastically move the piston downwards which dissipates energy much slower than the secondary unit. After a certain interval of time the piston rod cap will touch and rest on the surface of Mars that might relate to the balanced position of four novel hybrid legs.

## 8. Mechanical Design and Working

### a. Structural Configuration of Lander Leg

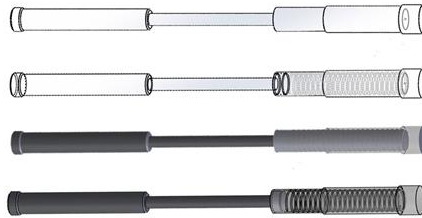


Fig.7 Typical design of lander leg

This novel shock absorber comprises of primary unit with hydraulic piston and secondary unit with helical compression spring. The secondary unit divides the cylinder into upper and lower compartment. Upper compartment is filled with compressed oil and air which are considered to be best adoptive methods for landers [13]. A control valve to release the hydraulic fluid and a pressure sensor is installed in the upper compartment. The work of the pressure sensor is to indicate the pressure to the control valve, when the pressure exceeds beyond predetermined level, it will send a signal to control valve to open and release the hydraulic fluid. Then, the hydraulic fluid will slowly move to another compartment. In addition to this we excogitated to install another hydraulic cylinder (tertiary) which is supposed to work when the pressure of the secondary unit exceeds beyond predetermined level.

### b. Lander Structure and Working



Fig.8 (a) Primary Structure (b) Secondary Structure

During terminal descent phase, when the lander is subjected to a vertical shock, the spring inside the primary unit is pressed downwardly. In this case, it will absorb maximum abrupt impact and store in the form of mechanical energy. After a certain period, it will transfer the same energy to the secondary unit obeying the newton's second law of motion which is alternatively defined by formula ( $F = - kx$ ). The mechanical energy which is transferred to secondary unit comprises of hydraulic cylinder with a piston rod. The piston rod is pressed upwardly so that the hydraulic system can absorb and dissipate the maximum shock. In this stage some small amount of hydraulic fluid will transfer from lower compartment to the upper compartment. When the impact shock exceeds beyond predetermined level, the pressure sensor will indicate the control valve to open and release the fluid to tertiary hydraulic compartment. After this stage, the piston rod in tertiary unit will move downwards due to pressure exerted by secondary unit. As a result, the lander will get rested on the surface of Mars.



Fig.9 Working of lander on Mars

## 9. Formulation

### a. Force exerted

Force exerted by the surface to the lander, at the time of hitting the ground

$$F_{exerted} = \frac{(2M(g - a) - C_d \rho v^2 A)}{2} \quad (\text{Unit} - kN)$$

**M** – Mass (**kg**), **g** – acceleration due to gravity of Mars (**m/s**), **a** – acceleration (**m/s**), **C<sub>d</sub>** – Drag coefficient, **ρ** – Mars atmospheric density (**kg/m<sup>3</sup>**), **v<sup>2</sup>** – square of the relative entry velocity (**m/s**), **A** – Base reference area (**m<sup>2</sup>**)

### b. Force absorbed

Total amount of impact force absorbed by primary leg of lander is derived from formula by [51]

$$F_{absorbed} = \left| -((P_p [d_1^2 - d_2^2] \times 0.785) - (P_1 A)) \times 10^{-3} \right| \quad (\text{Unit} - kN)$$

(-ve) sign indicates the absorption of force in negative direction.

**P<sub>p</sub>** – Pressure exerted by piston (**Pa**), **P<sub>1</sub>** – Pressure exerted by Hydraulic fluid (**Pa**),  
**d<sub>1</sub>** – Piston diameter (**mm**), **d<sub>2</sub>** – Piston rod diameter (**mm**), **A** – Piston area (**m<sup>2</sup>**)

### c. Force dissipated

Force dissipated by secondary legs towards positive direction is calculated from

$$F_{dissipated} = (P \times d_3 \times 0.785) \times 10^{-3} \quad (\text{Unit} - kN)$$

### d. Kinetic energy and speed

The Kinetic energy and speed of lander during hitting is calculated by using the formula

$$K.E = \frac{mv^2}{2} \quad (J)$$

Where **m** – mass of lander (**kg**), **v** – velocity (**m/s**)

$$\text{Speed}(v) = \sqrt{\frac{2}{m} K.E} \quad (\text{Unit} - m/s)$$

**K.E** – Kinetic energy (**joules**), **m**- mass of lander (**kg**)

## 10. Formulae

### a. Drag equation [29]

$$D = \frac{C_d \rho v^2 A}{2}$$

**C<sub>d</sub>** - Drag coefficient, **ρ** – Density of Mars Atmosphere, **V<sup>2</sup>** – Relative Entry Velocity, **A** – Reference Area

**C<sub>d</sub>** = 1.7 for 70° Spherical Cone Shell and **1.05** for 45° Spherical Cone Shell (**P. Subrahmanyam.et.al.2017**)

Density of Mars atmosphere **ρ** = ~**0.020 kg/m<sup>3</sup>** (**D.R. Williams.et.al.2016**) [30]



### b. Terminal Velocity

$$v_{terminal} = \sqrt{\frac{2W}{C_d \rho A}} \quad (\text{Unit} - m/s)$$

V - Terminal Velocity, W - Weight,  $C_D$  - Drag Coefficient,  $\rho$  - Gas Density, A - Frontal Area

### d. Ballistic coefficient

$$\beta = \frac{m}{C_d A} \quad (\text{Unit} - kg/m^3)$$

$\beta$  - Ballistic Coefficient, m - mass,  $C_D$  - Drag Coefficient, A - Reference Area

## 10. Aerodynamics

In aerodynamics, the geometry of aeroshell, diameter of parachute, entry velocity and ballistic coefficient determines the success rate of landing. From Viking era to the present generation, the geometry and mass factor is limited to 4.5m aeroshell diameter and 0.9-ton payload of mass (R.D. Braun et al. 2007). We cannot afford with current technology to land large scale mass in future Mars exploration missions, hence we need to increment the diameter of aeroshell as well as diameter of parachute. For large sized aeroshell, we require to improve our launch vehicle which will be more expensive. So, hypersonic inflatable aerodynamic decelerator is discussed to low down the terminal velocity and ballistic coefficient thereby increasing the drag force which might drastically reduce the terminal velocity.

### a. Mode of Entry

**Direct entry** - Direct mode of entry possesses high entry velocity and it will be difficult for faster aerocapture in a minimal interval of time. It has significant advantage of mass and simplest operations, but it does not provide design flexibility on Martian atmosphere such as dust storms [14]. Hence it might have highest probability of crash landing.

**Orbital entry** - Entry from orbit might diminish the entry velocity and enable us for effective preparation for Mars atmospheric entry. It is considered as one of the lowest risk and safest approach for manned landing [14]. Viking missions of NASA made their entry from Martian orbit and succeeded in soft-landing. Hence, orbital entry is expected to increase the probability of success.

**Selection of entry mode** - Our EDL follows vertical landing subsequent to the entry from Martian orbit. It terminates the perplexity in calibrating the orientation of the lander throughout the course of horizontal landing. This strategy is expected to save EDL time by thoroughly eliminating the lander's orientation program.

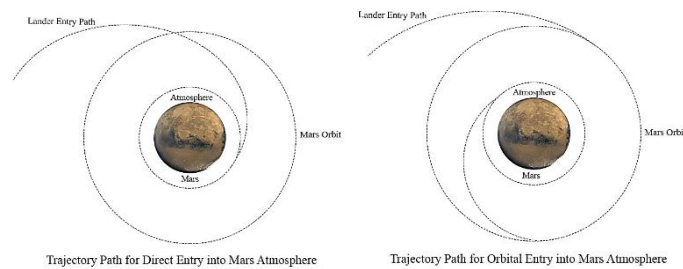


**Fig.10** Trajectory path for direct and orbital entry

### b. Hypersonic Inflatable Aerodynamic Decelerator Concept

For landing large scale masses, we need to increase the diameter of aeroshell described by (R.D. Braun.et.al.2007). To confront this need, we need to enhance our current launch vehicle which is expensive. To come across this necessity, it is desirable to utilize HIAD instead of enhancing launch vehicles as HIAD is emerging as one of the principal technology to faster aerocapture and landing large scale mass and crewed mission on the surface of Mars [15]. Currently, NASA's Langley Research Centre is investigating the development of HIAD to enable future human exploration mission. This type of HIAD can be employed to achieve faster aerocapture prior to landing within a short interval of time with  $L/D$  ranging from 0.2 to 0.5. A novel approach to HIAD and Aeroshell made of Flex shell is analyzed through Mars-GRAM simulation that has the capability of landing 20 metric tons of payloads with extensible diameter of aeroshell from 10m to 20m [16]. The use of HIAD is technologically feasible due to successful flight test of IRVE-II experiment and its technology development had been over viewed by Hughes.et.al.2011 [17].

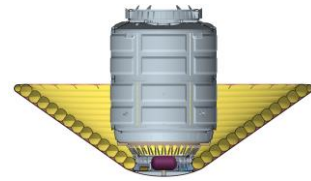


Fig.11 HIAD [19]

## 12. EDL Sequences

The complete EDL sequence follows four phases from its entry to ground touchdown. They are

- **Entry Phase** – from entry preparation to cruise stage separation
- **Hypersonic Phase** – from atmospheric entry to parachute deployment
- **Parachute Phase** – from peak deceleration to lander separation
- **Terminal Descent Phase** – from lander separation to ground touchdown

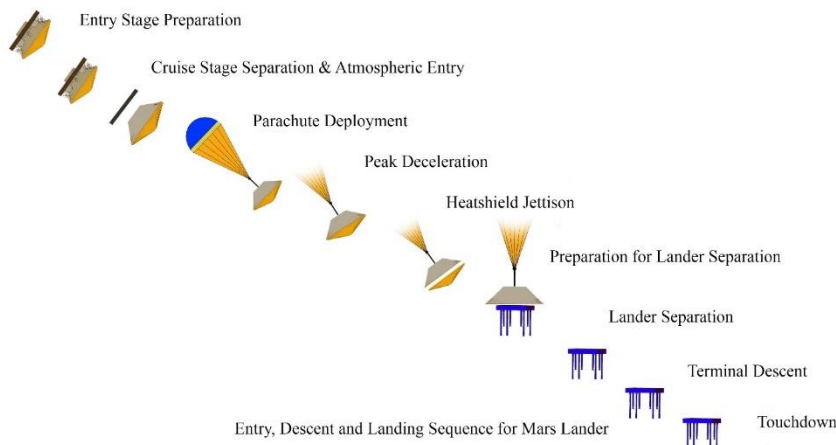


Fig.12 Entry, descent and landing sequence for Mars landers [50]

## 13. Entry, Descent and Landing Performance

### a. Entry

The descent vehicle is excoigitated to enter from Martian orbit to minimize the entry velocity in preference to direct entry. It is the safest approach for manned and large scale landing. This strategy eliminates the difficulties associated with dust storms that can be predicted well in advance by various Mars orbiters and acts as an early warning system for effective preparation for Mars atmospheric entry.

### b. Descent

The entry phase is followed by descent phase, where the lander undergoes fast aerocapture by the rapid action of parachute deployment and Hypersonic Inflatable Aerodynamic Decelerator. Using the Viking technology NASA had landed largest mass up to 900kg of Mars Science Laboratory. It used 70° Spherical cone shell with diameter of 4.5m. The need to increase the diameter of aeroshell in order to decrease the ballistic coefficient and faster aerocapture is limited due to the availability of launch vehicles. To overcome this situation Hypersonic Inflatable Aerodynamics Decelerators can be employed for faster aerocapture during descent phase.

### c. Landing

After successful descent, the lander undergoes landing where the novel legs will be deployed to rest the lander on the surface of Mars. Due to the effective design of lander, the legs in deployed position restrict the use leg deployment event. Our novel EDL follows vertical landing for un-deployable legs. Now the lander gets successfully descended on the surface.

## 14. Current EDL Challenges

Cargo and manned mission is fraught with new challenges like need for faster aerocapture prior to entry, requirement of large aeroshell diameter, limitation of large landing masses, rapid transition of entry, descent and landing sequence, the need for supersonic retropropulsion and increased system reliability [25]. Now the spacex has great capability of landing humans on Mars using Red Dragon hybrid capsule which uses supersonic retropropulsion. For powered descent Red Dragon requires 1900kg of propellant to decelerate from hypersonic phase to terminal descent phase for soft-landing on the surface of Mars [18]. Approaching this novel type of mechanical leg, it may reduce the mass of retropropulsive propellant thereby promoting cost efficient retropropulsive landing system for future manned missions.



**Fig.13** SpaceX Red dragon retropropulsive landing system [18]

## 15. Applications

This novel method of entry, descent and landing architecture will enable safe and large scale mass landings on the surface of Mars. It avoids the usage of expensive retropropulsive system thereby promoting cost effective landing on Mars. It has superior shock absorption capacity and the shock absorption capacity of novel leg varies according to the size, density of hydraulic fluid and the spring constant. This novel approach might have excellent applications in near future for human Mars exploration missions and large scale cargo missions. Some of the future proposals for lander mission under study are mentioned in the table-5, which explain the future prospects of this novel leg. A graph by (R. Biesbroek.et.al.2016) had shown the launch windows for future mars exploration missions which will be the best available technology for cost efficient launch and faster arrival at Mars.

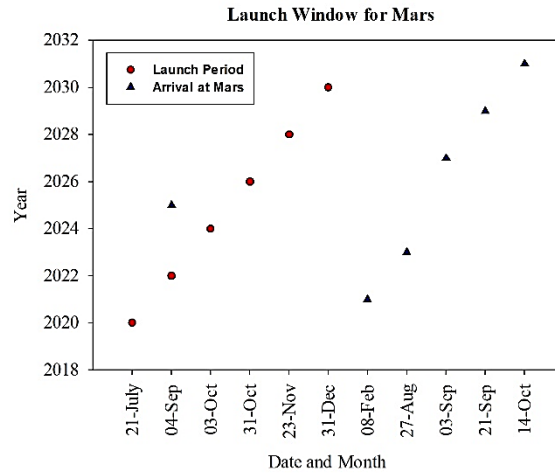


Fig.14 Launch windows for Mars

Table.3 Future lander proposals under study

Name	Country	Agency	Proposed Launch	Type	Ref
Mars MetNet Precursor	Finland	FMI	2018	Impact Lander	[20]
Mars MetNet	Finland	FMI	2018	Multi-Lander	[21]
Mars Geyser Hopper	Unites States	NASA	2018	Lander	[21]
Northern Light	Canada	CSA	2018	Lander   Rover	[22]
Icebreaker Life	United States	NASA	2018-20	Lander	[23]
Martian Moon Exploration	Japan	JAXA	2022	Lander   Sample Return	[24]
Phootprint	Europe	ESA	2024	Lander   Ascent Stage	[25]
Fobos-Grunt (Repeat)	Russia	ROSCOSMOS	2024	Lander   Ascent Stage	[26]
Mars-Grunt	Russia	ROSCOSMOS	2020	Orbiter   Lander	
BOLD	United States	NASA	2020	6 – Impact Landers	[27]
Mars Lander	South Korea	KARI	2020	Lander	[28]

## 16. Conclusions

In contrast to the crash incidences of past landers and the demand for future Mars exploration landing missions, novel approach to entry, descent and landing architecture is discussed and new theoretical design of landing gear is developed. Geometric and Aerodynamical approaches were described for faster aerocapture and to lower the ballistic coefficient. Additionally, EDL summary of past landers is compared and new formulations were done for shock attenuation. For this EDL system, vertical landing is preferred to horizontal landing due to time limiting factor. To effect perfect landing, the potential to inflatable aerodynamic decelerators and entry from orbit can be approached. In future, some of the proposed missions under study are tabulated with opportunity for future launch windows for Mars departure is as shown in the figure 16. The landing challenges for Mars landers were studied and some modifications were made to EDL sequences. This landing gear is technologically feasible for large scale and crewed landing on Mars. Simulation method for this model and prototype design will be studied further.

### Conflict of Interest:

The authors have no conflicts of interest to report.

### Funding:

No external funding was received to support this study.

### Acknowledgements

The author would like to thank Sir. Ahmed Sahinoz from Sabanci University, South Africa for providing Solidworks software packages.

### Subscripts:

G	-	Gravity ( $g = 9.8 \text{ m/s}^2$ for Earth and $3.71 \text{ m/s}^2$ for Mars) [49]
$C_d$	-	Drag coefficient
$\rho$	-	Density of Mars Atmosphere
D	-	Drag Force
V	-	Terminal Velocity
$\beta$	-	Ballistic Coefficient

### Nomenclature:

EDL	-	Entry, Descent and Landing
ESA	-	European Space Agency
EDM	-	Entry, Descent Module
NASA	-	National Aeronautics Space Administration
KARI	-	Korea Aerospace Research Institute
IRVE	-	Inflatable Re-entry Vehicle Experiment
FMI	-	Finnish Meteorological Institute
ROSCOSMOS	-	Russian State Corporation for Space Activities
CSA	-	Canadian Space Agency
JAXA	-	Japan Aerospace Exploration Agency
LEO	-	Low Earth Orbit
MPL	-	Mars Polar Lander
MPF	-	Mars Pathfinder
HIAD	-	Hypersonic Inflatable Aerodynamics Decelerator
L/D	-	Lift to drag ratio

### References

- [1] Musk, E. (2017). Making humans a multi-planetary species. *New Space*, 5(2), 46-61. doi.org/10.1089/space.2017.29009.emu.
- [2] Schroeder, K., Bayandor, J., & Samareh, J. A. (2016). Impact and Crashworthiness Characteristics of Venera Type Landers for Future Venus Missions. In *54th AIAA Aerospace Sciences Meeting* (p. 0221). doi.org/10.2514/6.2016-0221.
- [3] Holmberg, N. A., Faust, R. P., & Holt, H. M. (1980). Viking'75 spacecraft design and test summary. Volume 1: Lander design. Document ID- 19810001592.
- [4] Perminov, V. G. (1999). *The difficult road to Mars: a brief history of Mars exploration in the Soviet Union*. Document ID- 19990054835.
- [5] Braun, R. D., & Manning, R. M. (2007). Mars exploration entry, descent, and landing challenges. *Journal of spacecraft and rockets*, 44(2), 310-323. doi.org/10.2514/1.25116.
- [6] Moroz, V. I., Huntress, W. T., & Shevaley, I. L. (2002). Planetary missions of the 20th century. *Cosmic Research*, 40(5), 419-445. doi.org/10.1023/A:1020690700050.
- [7] Ferri, F., Ahondan, A., Colombatti, G., Bettanini, C., Bebei, S., Karatekin, O., & Forget, F. (2017, June). Atmospheric mars entry and landing investigations & analysis (AMELIA) by ExoMars 2016 Schiaparelli Entry Descent module: The ExoMars entry, descent and landing science. In *Metrology for AeroSpace (MetroAeroSpace), 2017 IEEE International Workshop on* (pp. 262-265). IEEE. doi:10.1109/MetroAeroSpace.2017.7999576.
- [8] Albee, A., Battel, S., Brace, R., Burdick, G., Casani, J., Lavell, J., ... & Dipprey, D. (2000). Report on the loss of the Mars Polar Lander and Deep Space 2 missions. Jet Propulsion Laboratory, California Institute of Technology. Document ID- 20000061966.
- [9] Golombek, M., Kipp, D., Warner, N., Daubar, I. J., Ferguson, R., Kirk, R. L., ... & Campbell, B. A. (2017). Selection of the InSight landing site. *Space Science Reviews*, 211(1-4), 5-95. doi.org/10.1007/s11214-016-0321-9.
- [10] Yamada, Y., & Kuwabara, T. (2007). A Guide to Spring Material Selection. In *Materials for Springs* (pp. 1-46). Springer Berlin Heidelberg. doi.org/10.1007/978-3-540-73812-1\_1. ISBN 978-3-540-73811-4.

- [11] Hunt, T. M., Hunt, T., Vaughan, N. D., & Vaughan, N. (1996). *The hydraulic handbook*. Elsevier. ISBN-1856172503, 9781856172509.
- [12] Brubaker, Jack (24 April 2017) "Hydraulic Oil Density" *Sciencing*. Retrieved from <https://sciencing.com/hydraulic-oil-density-6052242.html> on 24-06-2018.
- [13] Louis, B. C. M. (1955). *U.S. Patent No. 2,721,074*. Washington, DC: U.S. Patent and Trademark Office.
- [14] Wells, G. W., Lafleur, J. M., Verges, A., Manyapu, K., Christian III, J. A., Lewis, C., & Braun, R. D. (2006). Entry descent and landing challenges of human Mars exploration. Retrieved from <http://hdl.handle.net/1853/14772>.
- [15] Harper, B., & Braun, R. D. (2014). Asymmetrically Stacked Tori Hypersonic Inflatable Aerodynamic Decelerator Design Study for Mars Entry. In *AIAA Atmospheric Flight Mechanics Conference* (p. 1095). doi.org/10.2514/6.2014-1095.
- [16] Skolnik, N., Kamezawa, H., Li, L., Rossman, G. A., Sforzo, B., & Braun, R. D. (2017). Design of a Novel Hypersonic Inflatable Aerodynamic Decelerator for Mars Entry, Descent, and Landing. In *AIAA Atmospheric Flight Mechanics Conference* (p. 0469). doi.org/10.2514/6.2017-0469.
- [17] Hughes, S., Cheatwood, F., Dillman, R., Calomino, A., Wright, H., DelCorso, J., & Calomino, A. (2011, May). Hypersonic inflatable aerodynamic decelerator (HIAD) technology development overview. In *21st AIAA Aerodynamic Decelerator Systems Technology Conference and Seminar* (p. 2524). doi.org/10.2514/6.2011-2524.
- [18] Grover, M. R., Sklyanskiy, E., Stelzner, A. D., & Sherwood, B. (2012, June). Red dragon-msl hybrid landing architecture for 2018. In *Concepts and Approaches for Mars Exploration* (Vol. 1679). Retrieved from <http://adsabs.harvard.edu/abs/2012LPICo1679.4216G>.
- [19] Biesbroek, R. (2016). Transfer to a Planet. In *Lunar and Interplanetary Trajectories* (pp. 19-39). Springer, Cham. doi.org/10.1007/978-3-319-26983-2\_2.
- [20] Harri, A. M., Schmidt, W., Pichkhadze, K., Linkin, V., Vazquez, L., Uspensky, M., ... & Alexashkin, S. (2008, September). MPPM-Mars MetNet precursor mission. In *European Planetary Science Congress 2008* (p. 361). Bib code: 2008epsc.conf..361H Retrieved from <http://adsabs.harvard.edu/abs/2008epsc.conf.361H>.
- [21] Landis, G., Oleson, S., & McGuire, M. (2012, January). Design study for a mars geyser hopper. In *50th AIAA Aerospace Sciences Meeting including the New Horizons Forum and Aerospace Exposition* (p. 631). doi.org/10.2514/6.2012-631.
- [22] Quine, B., Lee, R., & Roberts, C. (2008). Northern light-a Canadian mars lander development plan. In *Conference Proceedings of CASI ASTRO*.
- [23] McKay, C. P., Stoker, C. R., Glass, B. J., Davé, A. I., Davila, A. F., Heldmann, J. L., ... & Paulsen, G. (2013). The Icebreaker Life Mission to Mars: a search for biomolecular evidence for life. *Astrobiology*, 13(4), 334-353. doi.org/10.1089/ast.2012.0878.
- [24] Miyamoto, Hirdly (17 March 2016). "Japanese mission of the two moons of Mars with sample return from Phobos" (PDF). NASA MEPAG. Retrieved from [http://mepag.nasa.gov/meeting/2016-03/17\\_Miyamoto.pdf](http://mepag.nasa.gov/meeting/2016-03/17_Miyamoto.pdf) on 16-06-2018.
- [25] Koschny, D., Svedhem, H., & Rebuffat, D. (2014). Phootprint-A Phobos sample return mission study. In *40th COSPAR Scientific Assembly* (Vol. 40). Bibcode: 2014cosp...40E1592K.
- [26] Zelenyi, L., Martynov, M., Zakharov, A., Korablev, O., Ivanov, A., & Karabadzak, G. (2014). Phobos Sample Return: Next Approach. In *40th COSPAR Scientific Assembly* (Vol. 40). Bib code: 2014cosp...40E3769Z. Retrieved from <http://adsabs.harvard.edu/abs/2014cosp...40E3769Z>.
- [27] Schulze-Makuch, D., Head, J. N., Houtkooper, J. M., Knoblauch, M., Furfaro, R., Fink, W., ... & Deamer, D. (2012). The Biological Oxidant and Life Detection (BOLD) mission: A proposal for a mission to Mars. *Planetary and Space Science*, 67(1), 57-69. doi.org/10.1016/j.pss.2012.03.008.
- [28] Lee, E. S., Chang, K. S., & Park, C. (2004). Design Study of a Korean Mars Mission. *International Journal of Aeronautical and Space Sciences*, 5(2), 54-61. doi.org/10.5139/IJASS.2004.5.2.054.
- [29] Benson, T. (2008). The drag equation. *NASA website*. Retrieved from <https://spaceflightsystems.grc.nasa.gov/education/rocket/drageq.html> on 01-07-2018.
- [30] Williams, D. R. (2004). Mars fact sheet. Retrieved from <https://nssdc.gsfc.nasa.gov/planetary/factsheet/marsfact.html> on 01-07-2018.
- [31] Benson, T. (2018). Terminal Velocity (gravity and drag). *NASA website*.
- [32] Meginnis, I. M., Putnam, Z. R., Clark, I. G., Braun, R. D., & Barton, G. H. (2013). Guided entry performance of low ballistic coefficient vehicles at Mars. *Journal of Spacecraft and Rockets*, 50(5), 1047-1059. doi.org/10.2514/1.A32425.
- [33] Williams, D. R. (27 November 2017) "Mars Page" *National Space Science Data Center*. Retrieved from <https://nssdc.gsfc.nasa.gov/planetary/planets/marspage.html> on 29-06-2018.
- [34] Williams, D. R. (21 March 2017) "Mars 2 – COSPAR ID -1971-045A , Mars 3 – COSPAR ID – 1971-049A , Mars 6 – COSPAR ID – 1973 – 052A , Mars 7 – COSPAR ID – 1973 – 053A , Viking-1 Lander – COSPAR ID – 1975-075C , Viking-2 Lander – COSPAR ID – 1975-083A , Mars Pathfinder – COSPAR ID – 1996-068A , Mars Polar Lander – COSPAR ID – 1999-001A , Deep Space 2 – COSPAR ID – DEEPS2 , Phoenix Mars Lander – COSPAR ID – 2007-034A" *NASA Space Science Data Coordinated Archive*. COSPAR ID - 1971-045A. Retrieved from <https://nssdc.gsfc.nasa.gov/nmc/> on 29-06-2018.
- [35] Subrahmanyam, P., & Rasky, D. (2017). Entry, Descent, and Landing technological barriers and crewed MARS vehicle performance analysis. *Progress in Aerospace Sciences*, 91, 1-26. doi.org/10.1016/j.paerosci.2016.12.005.
- [36] Vell, Edwin.V (11 April 2016) "Phobos Project Information" *National Space Science Data Center*. Retrieved from <https://nssdc.gsfc.nasa.gov/planetary/phobos.html> on 16-06-2018.
- [37] Nilsen, E. N. (2012). Exploring Mars: an overview.
- [38] Desai, P. N., Prince, J. L., Queen, E. M., Schoenenberger, M. M., Cruz, J. R., & Grover, M. R. (2011). Entry,

- descent, and landing performance of the Mars Phoenix Lander. *Journal of Spacecraft and Rockets*, 48(5), 798-808. doi.org/10.2514/1.48239.
- [39] Northey, D. (2003). The main parachute for the Beagle 2 Mars Lander. In *17th AIAA Aerodynamic Decelerator Systems Technology Conference and Seminar* (p. 2171). doi.org/10.2514/6.2003-2171.
- [40] Huntress, W. T., & Marov, M. Y. (2011). The last gasp: Mars-96. In *Soviet Robots in the Solar System* (pp. 387-405). Springer, New York, NY. doi.org/10.1007/978-1-4419-7898-1\_20.
- [41] Willcockson, W. H. (1999). Mars Pathfinder heatshield design and flight experience. *Journal of Spacecraft and Rockets*, 36(3), 374-379. doi.org/10.2514/2.3456.
- [42] Cruz, M., & Chadwick, C. (2000, August). A Mars Polar Lander Failure Assessment. In *Atmospheric Flight Mechanics Conference* (p. 4118). doi.org/10.2514/6.2000-4118.
- [43] Lindstrand, P. (2003). Parachute Subsystems for the Beagle 2 Mars Lander Entry Descent and Landing Systems. In *44th AIAA/ASME/ASCE/AHS/ASC Structures, Structural Dynamics, and Materials Conference* (p. 1902). doi.org/10.2514/6.2003-1902.
- [44] Linkin, V., Harri, A. M., Lipatov, A., Belostotskaja, K., Derbunovich, B., Ekonomov, A., ... & Nenarokov, D. (1998). A sophisticated lander for scientific exploration of Mars: scientific objectives and implementation of the Mars-96 Small Station. *Planetary and space science*, 46(6-7), 717-737. doi.org/10.1016/S0032-0633(98)00008-7.
- [45] Tolker-Nielsen, T. (2017). *EXOMARS 2016-Schiaparelli anomaly inquiry*. Report DG-I/2017/546/TTN, European Space Agency (ESA).
- [46] Van Hove, B., & Karatekin, Ö. Uncertainty analysis and Preliminary Reconstruction of the Mars Atmosphere using the ExoMars Schiaparelli Flush Air Data System. Retrieved on 26-09-2018.
- [47] Abilleira, F., Frauenholz, R., Fujii, K., Wallace, M., & You, T. H. (2014). 2016 Mars Insight Mission Design and Navigation. doi.org/10.1007/s11214-012-9892-2.
- [48] "InSight Lithograph" (PDF). NASA, July 2015. LG-2015-07-072-HQ. Retrieved from <http://www.jpl.nasa.gov/images/insight/InSightLitho2015.pdf>
- [49] Schenk, P. M., & Moore, J. M. (2000). Stereo topography of the south polar region of Mars: Volatile inventory and Mars Polar Lander landing site. *Journal of Geophysical Research: Planets*, 105(E10), 24529-24546. doi.org/10.1029/1999JE001054.
- [50] O'neal, M., Sabahi, D., & Tauber, M. (1998). *U.S. Patent Application No. 29/056,094*. (Aeroshell).
- [51] Bosch Rexroth (10 Jan 2013) "Formulary Hydraulics" *Rexroth – A Bosch Company*. Retrieved from [http://www.boschrexroth.co.in/business\\_units/bri/de/downloads/hyd\\_formelsammlung\\_en.pdf](http://www.boschrexroth.co.in/business_units/bri/de/downloads/hyd_formelsammlung_en.pdf) on 27-07-2018.
- [52] Smith, D. E., Zuber, M. T., Solomon, S. C., Phillips, R. J., Head, J. W., Garvin, J. B., ... & Lemoine, F. G. (1999). The global topography of Mars and implications for surface evolution. *Science*, 284(5419), 1495-1503. doi.org/10.1126/science.284.5419.1495.